2012 OSTST Meeting, Session of Instrument Processing
22-29 September 2012, Venice, Italy

Retracking Contaminated Altimetry Waveforms over Coastal and Inland Lake Regions

Kuo-Hsin Tseng[1,2], C.K. Shum[1], Yuchan Yi[1], Douglas E. Alsdorf[1], Hyongki Lee[3], Chungyen Kuo[4]

[1]Division of Geodetic Science, School of Earth Sciences, Ohio State University (tseng.95@osu.edu, ckshum@osu.edu, yi.3@osu.edu, alsdorf.1@osu.edu)
[2]College of Public Health, Ohio State University (1841 Neil Ave, 400 Cunz Hall, Columbus, Ohio, USA 43210)
[3]Dept. of Civil & Environmental Engineering, University of Houston (Houston, TX, USA, hlee@uh.edu)
[4]Department of Geomatics, National Cheng-Kung University (Tainan, Taiwan, kuo70@mail.ncku.edu.tw)

1. Summary

Innovative usage of satellite altimetry has enabled accurate observations of water level changes in small inland hydrologic bodies, and coastal sea-level variations. The innovation is based on advances in altimetry radar waveform retracking technique, in that robust identification is feasible for distinct leading edges for a variety of multi-peak pattern or distorted waveforms, due to land/ice contaminations or in regions of energetic ocean dynamics. Here, we demonstrate two novel techniques developed to mitigate either land or ice contaminated waveforms. When the satellite traverses across the ocean/lake shorelines or over ice, entering or leaving the water, the heterogeneous radar response could induce spurious peaks which migrate into the waveform patterns and lead to an overestimate of the telemetered range. Our first waveform modification, or Sub-waveform Filtering (SF) method is shown to be effective to mitigate overlapped peaks and yield improved Envisat altimetry ranges in 1-7 km offshore off various coastal study regions including seasonally sea-ice covered ocean near NE Greenland (Fig. 1). Our second method, the Track Offset Correction (TOC), is aimed at mitigating waveforms traversing from/to ice-covered boreal lakes to/from water, typically with a sharp leading edge and anomalously high power. Here we demonstrate this technique over the Qinghai Lake, Tibetan Plateau.

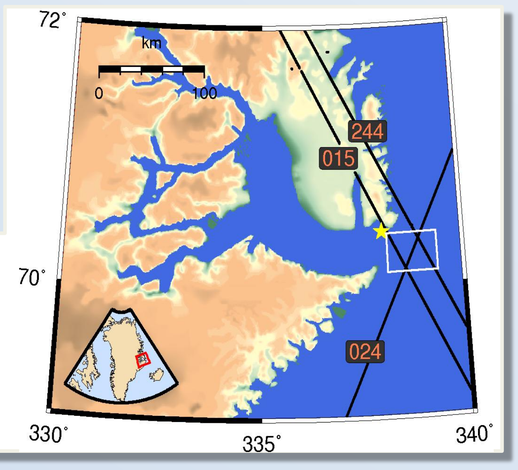

Figure 1. A study area picked to examine SF method near east Greenland. Black lines are Envisat passes and yellow star is the location of gauge station. Other study regions include: (1) Los Angeles, California, (2) Freshwater Canal Locks, Louisiana, (3) Cape May, New Jersey, and (4) Fort Myers, Florida.

2. Subwaveform Filtering (SF) Method

Waveforms at deeper ocean region (20~30km) are used for each altimeter pass as a reference (Eq.1) in this method to mitigate coastal (<7km) waveforms with erroneous or spurious peaks (Eq.2), which are induced from radar returns of non-water surfaces.

$$P_{ref}(i) = \frac{1}{k}\sum_{k=20\,km}^{30\,km} P_k(i) \quad , \quad i = \begin{cases} 1 \sim 128 \text{ for Envisat} \\ 1 \sim 104 \text{ for Jason-2} \end{cases} \tag{1}$$

where i = waveform gate, P_{ref} = reference waveform

k = number of waveforms between 20~30km from coasts

$$P_c(out) \in \left| P_c(i) - P_{ref}(i) \right| > 2\sigma \quad , \quad i = \begin{cases} 1 \sim 128 \text{ for Envisat} \\ 1 \sim 104 \text{ for Jason-2} \end{cases} \tag{2}$$

where P_c = coastal waveform (<7km), $P_c(out)$ = gate outliers in coastal waveform

σ = standard deviation of $P_c(i) - P_{ref}(i)$

The flawed waveform is then "repaired" by a 2D linear interpolation from neighboring gates, both in-waveform (adjacent gates) and along-track waveforms (same and diagonal gates in nearby measurements) (Eq.3).

$$\begin{aligned} \bar{P}_c(out) = \frac{1}{2\sqrt{2}+4}\{ & \left[P_c(out+1) + P_c(out-1) + P_{c+1}(out) + P_{c-1}(out) \right] \\ & + \frac{1}{\sqrt{2}} \left[P_{c+1}(out+1) + P_{c-1}(out-1) + P_{c+1}(out-1) + P_{c-1}(out+1) \right] \} \end{aligned} \tag{3}$$

where $\bar{P}_c$ = repaired coastal waveform

In addition, we apply an energy compensation correction for repaired waveform based on the reference waveform (Eq. 4).

$$\hat{P}_c(i) = \bar{P}_c(i) \times \sum_{i=a}^{b} P_{ref}(i) \Big/ \sum_{i=a}^{b} \bar{P}_c(i) \quad , \quad a = \begin{cases} 45 \\ 31 \end{cases} ; \; b = \begin{cases} 128 \text{ for Envisat} \\ 104 \text{ for Jason-2} \end{cases} \tag{4}$$

This correction is necessary because the total return energy is limited by the Automatic Gain Control (AGC) loop in the onboard altimeter. Once an extra high return signal existed in the waveform has been removed, the remaining bins following noise level are underestimated and need to be amplified to a similar level to the reference waveform. Finally, we compute an averaged height between 1~7km off the coastline for each pass and compare with tide gauge 6-minute water level data* nearby. * Data from NOAA (http://tidesandcurrents.noaa.gov/index.shtml)

3. Example Application of SF Method (Coastal Louisiana)

Fig. 2 demonstrates the SF method on Envisat data (cycle 91, pass 305) near Freshwater Canal Locks gauge station. Waveforms were contaminated by land at 7km offshore. An erroneous peak in 2D view of the stack waveforms shown (red curve, middle, upper corner) was migrated from the radar footprint edge (end of trailing edge) to nadir (nominal tracking gate #46). SF method mitigated the waveform (left panel).

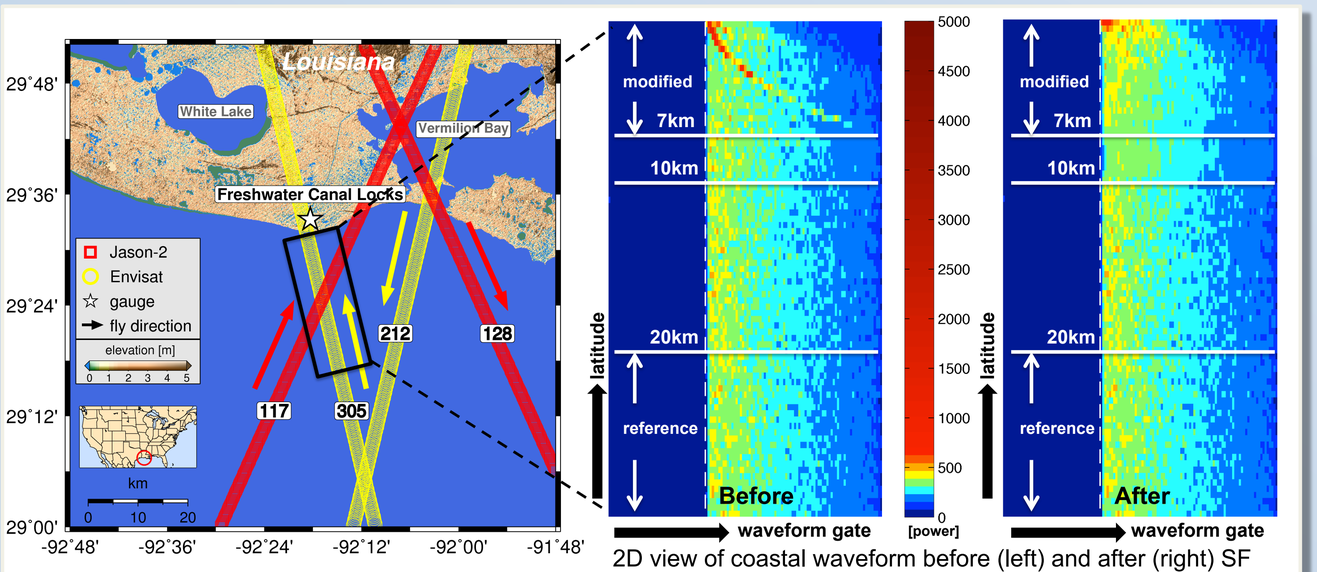

2D view of coastal waveform before (left) and after (right) SF

Figure 2. Waveform modification exemplified by Envisat pass near coastal Louisiana region

4. Track Offset Correction (TOC) for Boreal Lake Waveforms

Seasonal patterns of waveform shapes evident in Envisat measurements over the seasonally ice-covered boreal lake, Qinghai Lake on the Tibetan Plateau (Fig. 3).

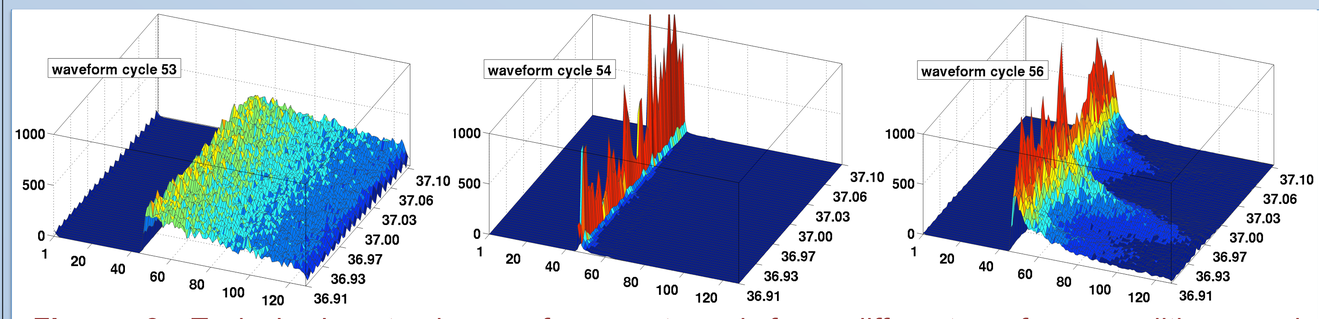

Figure 3. Typical along-track waveforms returned from different surface conditions and corresponding months: (**left**) water (Apr–Nov), (**middle**) ice (Dec–Mar), and (**right**) water with ice floes (Mar and Dec). X-axis is waveform gates (or bins), Y-axis is latitude in degree, and Z-axis is returned energy in power unit. These waveform samples are examples of Envisat pass #240 within cycles 53, 54, and 56 (from left to right).

The specular shape of waveform over frozen lake (Fig. 4) has steeper leading and trailing edges, thus shortens the telemetered range and yield a higher lake surface height retrieval applying the Threshold waveform retracker.

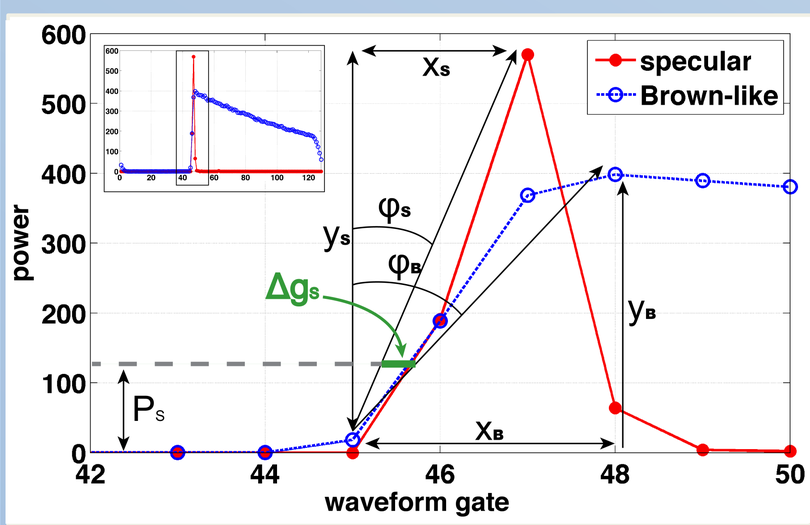

Figure 3. A conceptual illustration of TOC (Δg_s) demonstrated by a reference Brown-like shape measured over water and a specular shape waveform measured over frozen lake surface. An example (not to-scale) of power threshold (P_s, gray dashed line) meets two slopes at different gate in abscissa, as a retracked gate difference Δg_s (green) is observed during waveform retracking process.

Thus we introduce a TOC method to adjust the track offset error due to a shift of waveform peak leaning towards the front.

$$\Delta g_S = P_S \times (\tan\varphi_B - \tan\varphi_A) = P_S \times \left(\frac{x_B}{y_B} - \frac{x_S}{y_S}\right) \tag{5}$$

This correction in range is thus expressed as

$$R_S = R - \Delta g_S \times gm \tag{6}$$

where

R_s = retracked height after applying gate correction [m]

R = original 20% TR retracked height

gm = 0.4684375 (gate to meter conversion, based on 320 MHz bandwidth)

5. Results – SF Method

Table 1. (For four N. America cases) RMSE of different retrackers computed from Envisat and Jason-2 altimeters. Recommended retracker is highlighted in the entry of each zone.

Satellite and Retracker		1km-7km RMSE [cm]	0.5km-1km RMSE [cm]
Envisat	ICE-1	23	38
	OCEAN	35	48
	20%TR-SF	17	43
	20%TR-org	26	38
Jason-2	ICE	28	68
	OCEAN	86	*
	20%TR-SF	28	71
	20%TR-org	33	67
Overall	ICE/ICE-1	25	50
	OCEAN	56	*
	20%TR-SF	22	54
	20%TR-org	29	50

SF method works better in the 1-7 km offshore region than in 0.5–1 km.

Legend:
RMSE = root-mean-square error of retracked SSH time series;
20%TR-SF = 20% Threshold retracker using SF modified waveforms;
20%TR-org = 20% Threshold retracker using original waveforms
Correlation = correlation coefficient between retracked and gauge time series

* too many invalid cycles

Table 2. RMSE of available pass/cycles over east Greenland coastal region. Shaded cells indicate recommended retrackers based on the evaluation of RMSE and correlation against tide gauge data.

Pass		ICE-1	OCEAN	SEAICE	20%TR	20%TR SF
224	RMSE [cm]	21	41	42	22	17
	Correlation	0.77	0.5	0.42	0.76	0.87
	Cycle gap	0	4	0	0	0
24	RMSE [cm]	14	61	34	15	14
	Correlation	0.88	0.25	0.43	0.86	0.88
	Cycle gap	0	0	0	0	0
15	RMSE [cm]	30	72	62	30	23
	Correlation	0.58	0.43	0.42	0.58	0.71
	Cycle gap	0	0	0	0	0

SF method works fine while sea ice floes exist

Results – TOC Method

Table 3. RMSE and correlation coefficient compared among different retrackers and gauge data at Qinghai Lake.

Retracker	Pass #240 (lat: 36.90°N–37.10°N)		Pass #276 (lat: 36.73°N–36.79°N)	
	RMSE [cm]	Correlation	RMSE [cm]	Correlation
ICE-1	13±2	0.87	14±1	0.86
ICE-2	17±2	0.79	17±2	0.80
OCEAN	39±4	0.40	37±4	0.45
20% TR (uncorrected)	15±4	0.85	15±4	0.84
20%TR (TOC corrected)	6±7	0.98	6±7	0.97

Acknowledgement

The Ohio State University (OSU) component of this research is partially supported by a travel grant from NOAA/CIOSS, by NASA's Physical Oceanography and OSTST grants (NNX09AF42G and NNX08AR61G), by NASA's SWOT project (Doug Alsdorf), and by OSU's Climate, Water and Carbon program (http://cwc.osu.edu). The University of Houston (UH) component of this research is partially supported by UH's New Faculty Program.